Phys Chem Minerals (2001) 28: 211–217

ORIGINAL PAPER

D. Andrault · N. Bolfan-Casanova

High-pressure phase transformations in the $MgFe_2O_4$ and Fe_2O_3–$MgSiO_3$ systems

Received: 27 March 2000 / Accepted: 1 October 2000

Abstract The crystal structure of $MgFe_2O_4$ was investigated by in situ X-ray diffraction at high pressure, using YAG laser annealing in a diamond anvil cell. Magnesioferrite undergoes a phase transformation at about 25 GPa, which leads to a $CaMn_2O_4$-type polymorph about 8% denser, as determined using Rietveld analysis. The consequences of the occurrence of this dense $MgFe_2O_4$ form on the high-pressure phase transformations in the $(MgSi)_{0.75}(Fe^{III})_{0.5}O_3$ system were investigated. After laser annealing at about 20 GPa, we observe decomposition to two phases: stishovite and a spinel-derived structure with orthorhombic symmetry and probably intermediate composition between $MgFe_2O_4$ and Mg_2SiO_4. At pressures above 35 GPa, we observe recombination of these products to a single phase with Pbnm perovskite structure. We thus conclude for the formation of $Mg_3Fe_2Si_3O_{12}$ perovskite.

Key words Magnesioferrite · Spinel · Perovskite Phase transformation · X-ray Diffraction

Introduction

The spinel structure is adopted by many minerals of the upper Earth [for example, Fe_3O_4 magnetite in the crust; $MgAl_2O_4$ spinel in the upper mantle; $(Mg,Fe)_2SiO_4$ ringwoodite in the transition zone]. This is due to the fact that the structure can accommodate a large number of cations of different valences, and that these cations can disorder over the two different sites, tetrahedral and octahedral. This leads to a large number of solid solutions, such as, for example, $Fe_{3-x}Ti_xO_4$ titanomagnetites, which are important carriers of magnetism in the crust, or mantle spinels, which vary in composition between four end-member components (e.g., $MgAl_2O_4$, $FeAl_2O_4$, $MgCr_2O_4$ and $FeCr_2O_4$).

Spinel density is relatively low, because the presence of tetrahedral sites prevents compaction of the oxygen sublattice. It follows that the bulk modulus of spinels is high, with values between 165 and 240 GPa (Yutani et al. 1997), leading to phase transformations as pressure increases. AB_2O_4 compounds can be found with atomic arrangements denser than those of spinel, e.g. $CaFe_2O_4$ calcium-ferrite, $CaMn_2O_4$ marokite, and $CaTi_2O_4$ structure types. In these structure types the coordination around the cations is higher compared to spinel, and Ca is found in a dodecahedral site (CaO_8), whereas Fe, Mn, and Ti sit in octahedral sites. Also, a more compact three-dimensional network is formed by edge- and corner-sharing octahedra, with hollow channels parallel to the *c* axis, where the Ca cations are located. Differences between these denser structures lie in slight modifications of the polyhedral linkage, which result in the presence of two types of FeO_6 octahedra in $CaFe_2O_4$, a very distorted (and unique) MnO_6 site in $CaMn_2O_4$, and a more symmetric CaO_8 polyhedron in $CaTi_2O_4$ compared to $CaFe_2O_4$ and $CaMn_2O_4$ structures.

High-pressure phase transformations from spinel to one of these forms have been observed for Mn_3O_4, Fe_3O_4, $MgAl_2O_4$, $CaAl_2O_4$, and $(Mg_{0.1},Ca_{0.9})Al_2O_4$ (see Table 1). In particular, a phase transformation of Fe_3O_4 from spinel to $CaMn_2O_4$-type structure was reported above 23.6 GPa at 830 °C by Fei et al. (1999). This observation is closely related to the results of our study, which is partially devoted to the high-pressure behavior of $MgFe_2O_4$. The ultimate step of the spinel compression can lead to a breakdown of the AB_2O_4 stoichiometry into oxides, as observed for $MgAl_2O_4$ and Mg_2SiO_4 which decompose into $MgO + Al_2O_3$ and $MgO + MgSiO_3$, above 15 and 23 GPa, respectively (Liu 1975). However, at 25 GPa and higher temperatures (above

D. Andrault (✉)
Laboratoire des Géomatériaux, IPGP,
4 place Jussieu, 75252 Paris, France
e-mail: andrault@ipgp.jussieu.fr
Tel.: +33 1 44 27 48 89; Fax: +33 1 44 27 24 87

N. Bolfan-Casanova
Bayerisches Geoinstitut, Universität Bayreuth,
95440 Bayreuth, Germany
Now at Laboratoire des Géomatériaux, IPGP

Table 1 High-pressure phase transformation of compounds with the spinel structures. $CaMn_2O_4$ and $CaFe_2O_4$ are distorted forms of $CaTi_2O_4$, with octahedral and dodecahedral sites instead of tetrahedral and octahedral sites in spinel. All syntheses were performed at high temperatures

Composition	Structure at high *P*	Pressure of transformation	Reference
Mn_3O_4	$CaMn_2O_4$	10 GPa	Reid and Ringwood (1969)
Fe_3O_4	$CaMn_2O_4$	23.6 GPa, 823 K	Fei et al. (1999)
$MgFe_2O_4$	$CaMn_2O_4$	25 GPa[a]	This study
$CaAl_2O_4$	$CaFe_2O_4$	10 GPa	Reid and Ringwood (1969)
$CaAl_2O_4$	$CaFe_2O_4$	9 GPa, 1400 °C	Akaogi et al. (1999)
$MgAl_2O_4$	$CaFe_2O_4$	25 GPa	Irifune et al. (1991)
$MgAl_2O_4$	$CaFe_2O_4$	26.5 GPa, 1600 °C	Akaogi et al. (1999)
$MgAl_2O_4$	$CaTi_2O_4$	40 GPa[a]	Funamori et al. (1998)
$(Mg_{0.1},Ca_{0.9})Al_2O_4$	$CaFe_2O_4$	20–21 GPa	Akaogi et al. (1999)
$(Mg_{0.7},Ca_{0.33})Al_2O_4$	Hexa-form	15 GPa	Akaogi et al. (1999)

[a] Using laser annealing

1000 °C), Irifune et al. (1991) observed that $MgAl_2O_4$ adopted the $CaFe_2O_4$ structure. In addition, Funamori et al. (1998) observed that $MgAl_2O_4$ transforms to a $CaTi_2O_4$ structure above 40 GPa. In the first part of this paper we will present our results on the high-*P* phase transformation of $MgFe_2O_4$, and, in the second part, we will describe the chemical reactions between $MgSiO_3$ and Fe_2O_3 under (*P*, *T*) conditions of the transition zone and lower mantle.

Experiments

Two different starting materials were used for the high-pressure and high-temperature experiments: (1) an oxide mixture of MgO and Fe_2O_3 with $MgFe_2O_4$ bulk composition, and (2) a mixture of enstatite glass and hematite with $(MgSi)_{0.75}(Fe)_{0.5}O_3$ bulk composition. A small amount of Pt was added to the $MgSiO_3$ + Fe_2O_3 powder. A very thin gold foil was added to the magnesioferrite sample to infer the pressure in the sample chamber from gold *P–V* equation of state (EOS) (Anderson et al. 1989). We used a membrane-type DAC mounted with 300 μm culet diamonds. Samples were loaded in 100-μm-diameter holes drilled in preindented Re gaskets. After each pressure increase, samples were heated with a defocused, multimode YAG laser for which the central part of the temperature gradient was about 30 μm in diameter. Great care was taken to scan the hot spot slowly over the entire sample, thus allowing each part of the sample chamber to be heated to the maximum temperature for several seconds (Andrault et al. 1998a).

Angle-dispersive X-ray diffraction spectra were recorded at the ID30 beamline of the European Synchrotron Radiation Facility (ESRF, Grenoble, France). A channel-cut, water-cooled monochromator was used to produce a bright, monochromatic X-ray beam at 0.3738 Å wavelength. Vertical and horizontal focusing were achieved by bent-silicon mirrors, whose curvatures were optimized to obtain all X-rays in a 25 × 30 μm spot on the sample (Häusermann and Hanfland 1996; Andrault et al. 1998a). Two-dimensional images were recorded on an imaging plate in less than 5 min, and read online by the Fastscan detector (Thoms et al. 1998). Diffraction patterns were integrated using the Fit2d code (Hammersley 1996) and Lebail and Rietveld refinements were performed using the GSAS program package (Larson and Von Dreele 1998).

Results and discussion

High-pressure phase transformation of $MgFe_2O_4$

We first recorded diffraction patterns in the $MgFe_2O_4$ system as a function of pressure up to 46 GPa. Selected

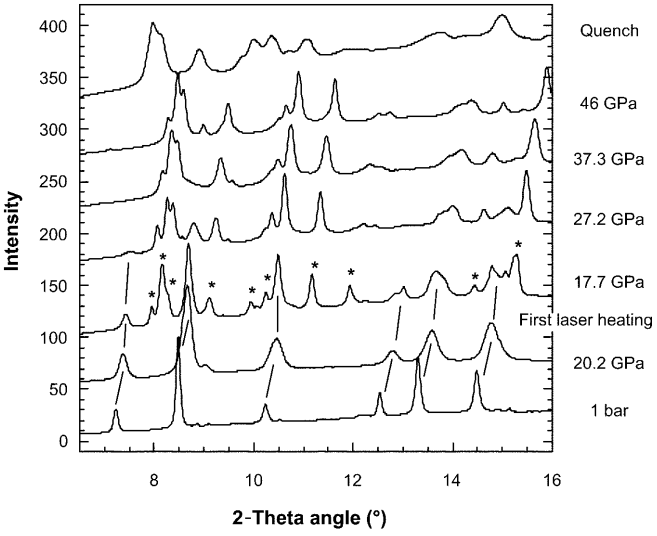

Fig. 1 Pressure evolution of $MgFe_2O_4$ X-ray diffraction patterns. New diffraction lines (*) occur at 17.7 GPa after the first laser heating. Above this pressure, reported pressures are for spectra recorded after YAG laser annealing at about 2500 K. Diffraction lines of the starting material are no longer visible above 27.2 GPa

spectra of the sample after laser annealing are reported in Fig. 1. We observe a phase transformation after the first laser annealing at 20.2 GPa. After quenching the temperature, the sample is found at a slightly lower pressure of 17.7 GPa, and shows new diffraction lines that are not explained by spinel-type magnesioferrite. This indicates the onset of a phase transformation to another polymorph. Still, the diffraction lines of spinel-type magnesioferrite remain clear up to 27.2 GPa, evidencing a mix of low-*P* and high-*P* phases between 17.7 and 27.2 GPa. The coexistence of the two polymorphs in an extended pressure range can be due to either the lack of pressure control during laser heating or temperature gradients. Note that (1) higher pressures are found in the central part of the laser hot spot due to thermal pressure effects (Andrault et al. 1998b), and (2) a phase transformation is followed by a decrease in volume, thereby causing a local pressure drop. We thus estimate the pressure of the phase transformation to be about 25 ± 3 GPa. No other phase is observed up to the maximum pressure of 46 GPa. The

high-*P* polymorph does not transform back to spinel-type magnesioferrite upon decompression. A clear line-broadening, however, suggests partial loss of long-range order (i.e., partial amorphization).

We selected the diffraction pattern recorded at 37.3 GPa for Rietveld analysis of the high-*P* polymorph, because the diffraction lines of spinel-type magnesioferrite are no longer present. Diffraction features perfectly match the $CaMn_2O_4$-type structural model (see Fig. 2), in a way identical to that previously proposed by Fei et al. (1999) for the high-*P* polymorph of Fe_3O_4. We find at 37.3 GPa a Pbcm orthorhombic lattice with [2.7392(5), 9.200(3), 9.285(2)] cell parameters and atomic positions as reported in Table 2. Atomic parameters are found close to but different from those of the high-*P* form of Fe_3O_4. The dodecahedral MgO_8 site shows four smaller and four larger MgO bonds, a 4 + 4 configuration that can be compared with the MgO_{12} dodecahedral 4 + 4 + 4 configuration found in $MgSiO_3$ perovskite. The octahedral $Fe^{III}O_6$ site appears highly distorted, with five bonds between 1.71 and 2.1 Å and a sixth one at 2.46 Å. Such a distortion is similar to that reported for the high-*P* form of Fe_3O_4 (Fei et al. 1999). A structure model is presented in Fig. 3. Edge linkage between adjacent $Fe^{III}O_6$ octahedra and MgO_8 dodecahedra makes this structure more compact than spinel, where octahedra form edge-sharing chains linked by isolated tetrahedra.

Cell parameters and volumes for the low-*P* and high-*P* polymorphs of $MgFe_2O_4$ polymorphs are reported in Table 3 and Fig. 4. Volumes for the high-*P* form are particularly accurate as stresses were released after YAG laser annealing to about 2500 K. However, the pressure measurements become less accurate as pressure increases, because the diffraction lines of gold (used as pressure standard) partially overlap with those of the sample. The high-*P* polymorph is found about 8% denser than spinel-type magnesioferrite at the transition pressure. The experimental volumes recorded between 18 and 46 GPa for high-*P* magnesioferrite indicate $V_0 = 558(7)$ Å^3, and $K_0 = 142(14)$ GPa, for fixed K' (using Birch-Murnaghan equation of state). For the low-*P* spinel form, we calculated $K_0 = 195(17)$ GPa, for K' fixed to 4, using only the diffraction patterns recorded after laser annealing (see Fig. 4). This value is lower than $K_0 = 233(40)$, $K' = 4.1(2)$, reported by Gerward and Ohen (1995), for magnesioferrite pressurized up to 37 GPa at room *T*. Nevertheless, our results are compatible with the value of 190 GPa, estimated from the $K_0 = f(V_0)$ general trend proposed for spinels by Yutani et al. (1997). It is also close to the value of $K_0 = 175.5$, $K' = 4$ reported by Woodland et al. (1999) for a set of spinels in the Fe_3O_4–Fe_2SiO_4 solid solution.

It is noticeable that the low-*P* form exhibits a higher bulk modulus than the high-*P* form of $MgFe_2O_4$. This unusual behavior could be due to the presence of

Table 2 Refined unit-cell and atomic positional parameters for the $CaMn_2O_4$-type phase of $MgFe_2O_4$ at 37.3 GPa

Space group: Pbcm; Z = 4
a = 2.7392(5) Å, *b* = 9.200(2) Å, *c* = 9.285(2) Å

Atom	Wyck	*x*	*y*	*z*
Mg	4d	0.731(11)	0.367(23)	1/4
Fe^{3+}	8e	0.291(3)	0.116(9)	0.084(7)
O1	4c	0.732(20)	1/4	0
O2	4d	0.235(28)	0.256(4)	1/4
O3	8e	0.000(5)	0.455(18)	0.117(1)
Mg-O1	2.561(9)	[2]	Fe-O1	2.11(4)
Mg-O2	1.71(7)	[1]	Fe-O1	1.895(34)
Mg-O2	1.72(5)	[1]	Fe-O2	2.008(19)
Mg-O3	2.486(25)	[2]	Fe-O3	1.713(16)
Mg-O3	1.647(18)	[2]	Fe-O3	2.463(18)
			Fe-O3	2.135(14)

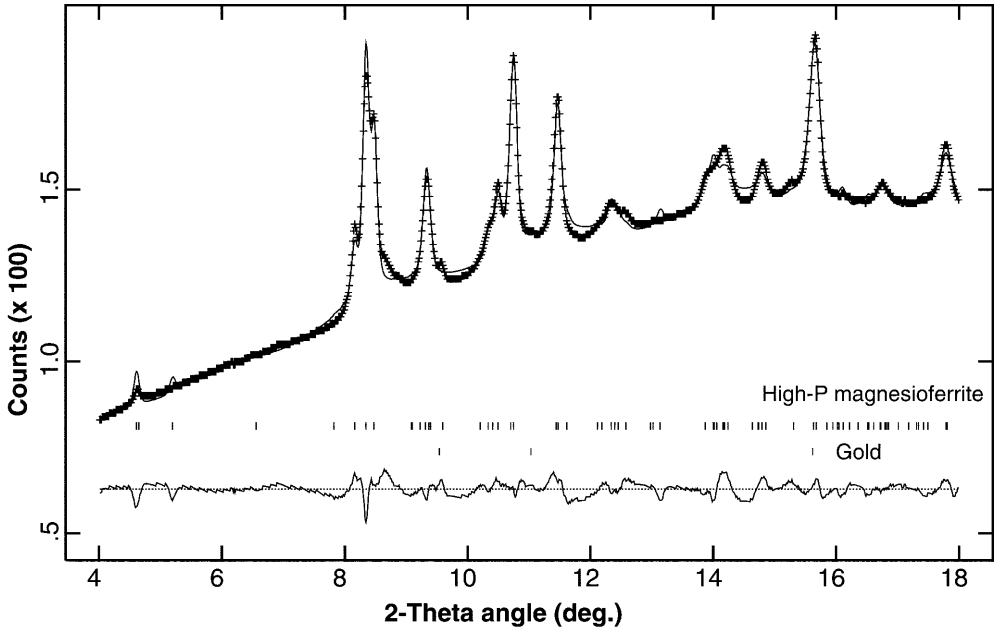

Fig. 2 Rietveld refinement of $MgFe_2O_4$ diffraction pattern recorded at 37.3 GPa after YAG laser annealing. The structure of the high-*P* polymorph of magnesioferrite is a $CaMn_2O_4$-type Pbcm orthorhombic lattice, with cell and atomic parameters as reported in Table 2. *Upper and lower ticks* correspond to the new $MgFe_2O_4$ phase and gold, respectively

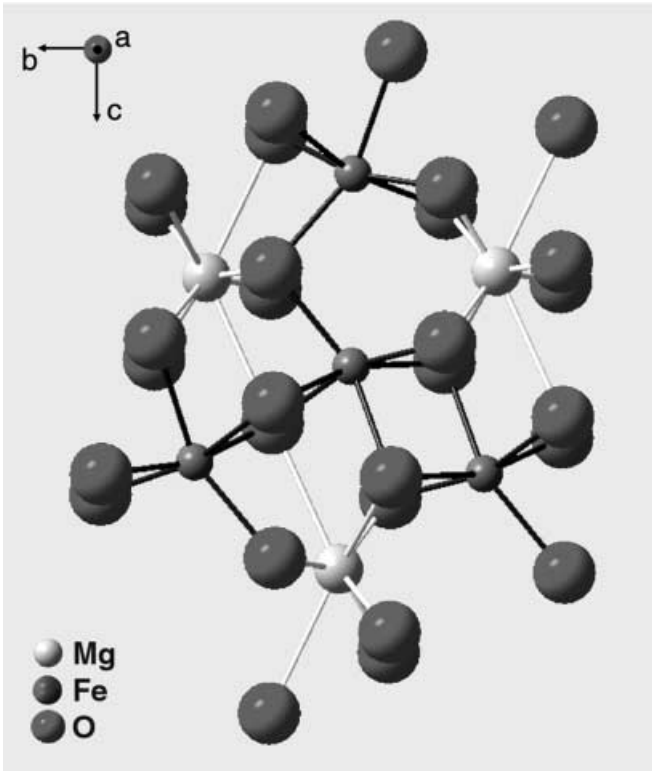

Fig. 3 High-*P* form of $MgFe_2O_4$ ($CaMn_2O_4$-type structure). Note the presence of Mg in the eight-coordinated site, and the edge-linkage between $Fe^{III}O_6$ octahedra. As for magnesioferrite, the oxygen sublattice remains a distorted face-centered stacking

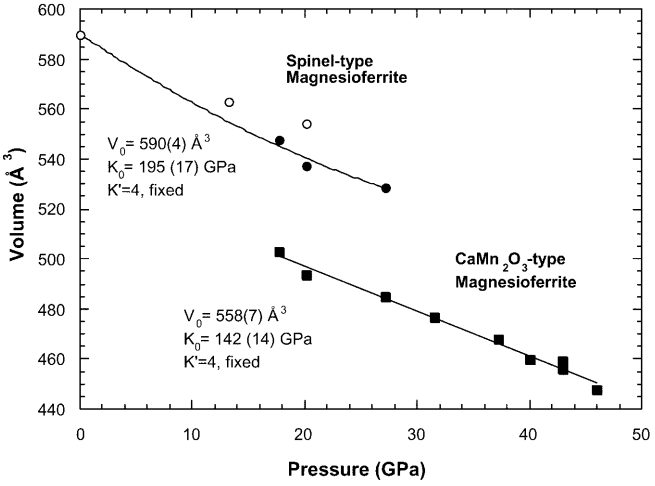

Fig. 4 Equation of state of the low-*P* spinel-type and high-*P* $CaMn_2O_4$-type polymorphs of $MgFe_2O_4$, showing a clear volume discontinuity of about 8% at about 20 GPa. *Full symbols* correspond to patterns recorded after laser heating

tetrahedral sites in the spinel structure, that are often little compressible. The low compressibility of the low-*P* form could be responsible for the rapid phase transformation to the $CaMn_2O_4$ form.

A spinel-type structure for $MgFe_2O_4$–Mg_2SiO_4 at ~20 Gpa

We then investigated the phase relationships in the $(MgSi)_{0.75}(Fe)_{0.5}O_3$ composition. We pre-compressed the sample to 27 GPa, according to the Pt EOS (Jamieson et al. 1982) and then laser-heated the sample to about 2500 K. Significant changes in the diffraction pattern were observed for the quenched sample, as shown in Fig. 5. We first note that the most intense diffraction lines of hematite, expected around 2.5 and 2.7 Å, are not observed. As no other Fe_2O_3 polymorph is expected at such a moderate pressure (Yagi and Akimoto 1982; Staun Olsen et al. 1991), this suggests a chemical reaction between Fe_2O_3 and $MgSiO_3$. Another important feature is the major diffraction line found at about 2.88 Å, characteristic of stishovite (110 line). According to the stishovite EOS (Andrault et al. 1998a), the pressure of the recovered sample is then ~20 GPa, evidencing a pressure release during laser annealing.

The fact that we observe such a high-intensity line for stishovite indicates substantial decomposition of $MgSiO_3$ into stishovite plus an Mg-enriched compound, Mg_2SiO_4 or MgO. Around similar (*P*, *T*) conditions, $MgSiO_3$ is known to decompose to a mixture of

Table 3 Unit cell parameters of the low-*P* and high-*P* forms of $MgFe_2O_4$ from ambient pressure to 46 GPa

P (GPa)	Spinel type		$CaMn_2O_4$ type			
	a (Å)	*V* (Å^3)	*a* (Å)	*b* (Å)	*c* (Å)	*V* (Å^3)
1.00e-05[a]	8.387(1)	589.9(3)				
13.3[a]	8.256(3)	562.7(6)				
20.2[a]	8.215(3)	554.3(6)				
17.7	8.180(8)	547.4(16)	2.812(3)	9.411(2)	9.506(1)	503.11(34)
20.2	8.130(13)	537.4(27)	2.792(3)	9.359(2)	9.448(2)	493.78(38)
27.2	8.086(23)	528.7(46)	2.774(3)	9.302(1)	9.389(2)	484.63(35)
31.6			2.759(5)	9.237(3)	9.353(2)	476.63(61)
37.3			2.739(5)	9.200(3)	9.285(2)	467.98(67)
43.0			2.723(5)	9.140(3)	9.225(2)	459.11(66)
40.0			2.724(5)	9.146(2)	9.230(2)	459.89(59)
43.0			2.717(5)	9.120(3)	9.201(2)	456.07(62)
46.0			2.701(5)	9.057(3)	9.155(2)	447.94(64)

[a] Data recorded without laser annealing

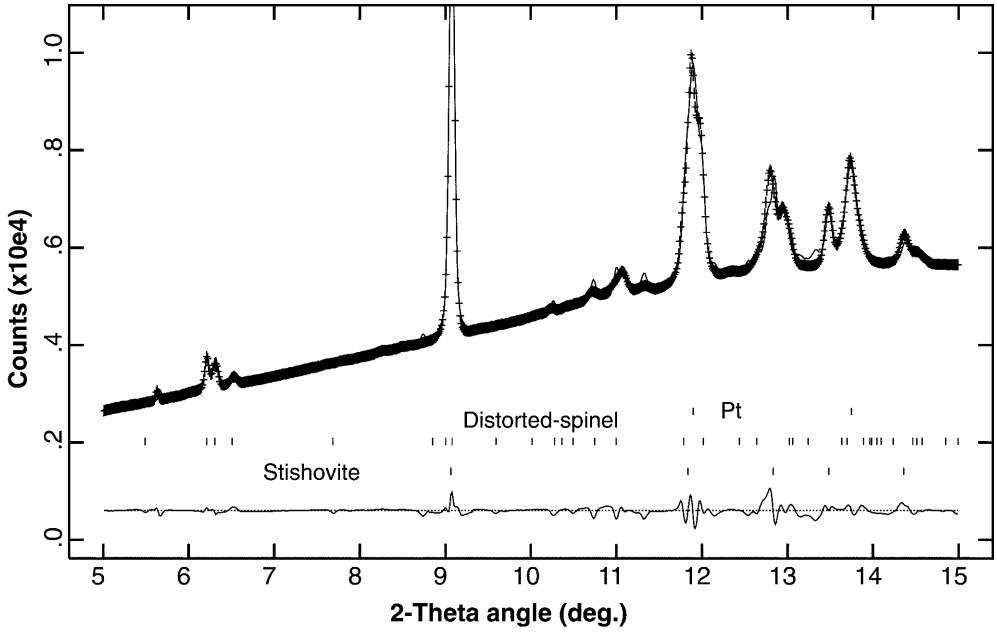

Fig. 5 Lebail refinement of the diffraction pattern obtained at 20 GPa after YAG laser annealing in the $(Fe_2O_3)_{0.25}(MgSiO_3)_{0.75}$ system. The main diffraction peak located around 2.88 Å (close to 9° 2-tetha) evidences the presence of stishovite. All diffraction features can be explained by the presence of stishovite and another compound, having a spinel-derived structure and a composition intermediate between Mg_2SiO_4 and $MgFe_2O_4$ (see text)

stishovite and Mg_2SiO_4 wadsleyite or ringwoodite, depending on experimental pressure and temperature (Ito and Takahashi 1989). However, the main diffraction lines of γ-Mg_2SiO_4 ringwoodite ($d_{111} = 4.74$ Å and $d_{311} = 2.48$ Å at room P), or β-Mg_2SiO_4 wadsleyite ($d_{112} = 2.62$ Å and $d_{141} = 2.44$ Å at room P) are not observed. The major diffraction lines of $MgFe_2O_4$ low-P and high-P forms are also not visible (around 2.47 and 2.63 Å, respectively; see Fig. 1). We thus conclude for the formation of a new phase, possibly following a chemical reaction such as that shown below:

$$0.25Fe_2O_3 + 0.75MgSiO_3 \Rightarrow \left[(MgFe_2O_4)_{0.25}(Mg_2SiO_4)_{0.25}\right] + 0.5SiO_2 \quad \text{at } 20\,\text{GPa} \ .$$

The occurrence of such an $[(MgFe_2O_4)_x(Mg_2SiO_4)_y]$ compound explains the formation of stishovite, and the absence of diffraction features characteristic of hematite, magnesioferrite, and β or γ phases of olivine.

Apart from the diffraction lines of Pt and stishovite, experimental features can be explained by an orthorhombic lattice, with unit-cell parameters of 8.417(2), 8.280(1), and 8.030(2). This lattice resembles that of a distorted spinel, with unit-cell parameters closely related to those of Mg_2SiO_4-ringwoodite, Fe_2SiO_4-spinel, and $MgFe_2O_4$-magnesioferrite cubic end members, with values of 8.220, 8.234, and 8.387 Å at room pressure, respectively. We do not have sufficient experimental constrains to perform a full refinement of this structure, because various space groups can explain the data. We note the presence of 200, 020, 002, 222, 004 Bragg lines, and of at least one line between (103, 013) and (321, 213, 312, 132) d_{hkl} lines (see Table 4). We propose a Lebail refinement using arbitrarily the Amaa space group (Fig. 5), but Pnnn, Imma, and Immm space groups are also possible. A similar spinel-type lattice with $a = 8.2797$ Å, $b = 8.2444$ Å, and $c = 8.1981$ Å was previously proposed for the low-temperature form of $LiMn_2O_4$ (Oikawa et al. 1998). Low-intensity diffraction lines at about 2.35 and 2.0 Å suggest the presence of trace amounts of another phase in the sample (possibly silicate perovskite, wadsleyite, or ringwoodite).

Mg–Si disorder seems to be very limited in ringwoodite, as observed by Hazen et al. (1993), who measured only 4% of the Si entering the octahedral site. The higher temperatures achieved in this study are likely, however, to promote higher Mg and Si disordering. In $MgSiO_3$ majorite, for example, one fourth of the Mg and Si share the octahedral site. The behavior of the solid solution between Mg_2SiO_4 and $MgFe_2O_4$ is still difficult to predict. From the inferred chemical composition of the newly formed compound, $Mg_{1.5}Fe_{1.0}Si_{0.5}O_4$, which we can rewrite as $(Mg,Fe)_2(Mg,Si)O_4$, an explanation would be that Mg and Si are disordered in one crystallographic site, whereas Mg and Fe are disordered in another. However, we cannot rule out the occurrence of Si–Fe disorder, as it certainly occurs in the mixed-spinel phase between Fe_3O_4 and Fe_2SiO_4, recently reported above 9 GPa and 1200 °C (Ohtaka et al. 1997).

Table 4 Bragg lines positions for distorted spinel-like structure of $(Mg,Fe)_2(Mg,Si)O_4$ (Fig. 5). d_{hkl} indexes suppose an orthorhombic lattice (see text)

dhkl (Å)	hkl
4.210	200
4.141	020
4.010	002
2.55	103, 103
2.381	222
≈2.20	321, 132, 213...
2.022	004

$Mg_3Fe_2Si_3O_{12}$ perovskite above 30 GPa

After further compression above 30 GPa of the sample synthesized in the $(MgSi)_{0.75}(Fe)_{0.5}O_3$ composition, the spinel-derived structure is no longer observed, as evidenced by disappearance of its characteristic diffraction lines at about 4.1 Å. We also observe a clear decrease with pressure of the relative intensity of the (110) line of stishovite. Finally, we note that the main diffraction lines of hematite and $CaMn_2O_4$-type $MgFe_2O_4$ are not present. Instead, at about 63 GPa after YAG laser annealing at about 2500 K, all diffraction features can be explained by a mixture of a Pbnm silicate perovskite, traces of stishovite, and platinum (Fig. 6). At this pressure, we recorded several diffraction patterns at different locations in the DAC, using the 30-μm diameter X-ray beam. Perovskite diffraction features are dominant, and stishovite lines are observed with varying intensity. This evidences an efficient reaction between SiO_2 and the spinel-derived structure observed at 20 GPa (Fig. 5). As no hematite and magnesioferrite features are observed in the diffraction patterns, our results indicate the formation of a perovskite compound with composition close to $Mg_3Fe_2Si_3O_{12}$, in a manner similar to that observed by Wang et al. (1999) for $Ca_3Fe_2Si_3O_{12}$ composition. After pressure release, we find $a = 4.803(6)$ Å, $b = 4.927(2)$ Å, $c = 6.897(4)$ Å, and $V = 162.74(9)$ Å^3 for the cell parameters of the perovskite phase. The volume is close to that of $MgSiO_3$ perovskite at room P (162.30 Å^3), but the (a, b, c) cell parameters, and thus the distortion of the orthorhombic cell are found to be significantly different.

Our result seems to contrast with those of McCammon et al. (1992) and Lauterbach et al. (2000), who observed that at ~25 GPa pure $(Mg,Fe)SiO_3$ perovskite dissolves very little ferric iron [$(Fe^{3+}/\Sigma Fe) \sim 5\%$] in the absence of aluminum. However, Staun Olsen et al. (1991) reported a phase transition of Fe_2O_3 into orthorhombic (Pbnm) perovskite structure at 55 GPa. Thus, it is possible that the higher pressures and temperatures experienced by our samples enhanced solid solution between $MgSiO_3$ and Fe_2O_3 perovskite end members. We also note that our experiments were performed at high SiO_2 activity (see Fig. 6), which was not the case for the multianvil experiments.

Conclusion

We report a new dense $CaMn_2O_4$-type polymorph of $MgFe_2O_4$ synthesized above 20 GPa at high temperature (> 2000 K). This phase was not observed in experiments performed under similar conditions but in an Si-bearing system of $(MgSi)_{0.75}(Fe)_{0.5}O_3$ bulk composition. Instead, our results indicate the formation of a spinel-type structure with composition intermediate between $MgFe_2O_4$ and Mg_2SiO_4 at about 20 GPa and high temperature. As Fe_3O_4 was previously reported to form a solid solution with Fe_2SiO_4-spinel (Ohtaka et al. 1997), we propose that a similar reaction occurs between $MgFe_2O_4$ and Mg_2SiO_4. It is thus likely that ferric iron dissolves into $(Mg,Fe)_2SiO_4$ ringwoodite in the Earth's transition zone.

At higher pressure (63 GPa), only perovskite and traces of stishovite are observed in the $(MgSi)_{0.75}(Fe)_{0.5}O_3$ system. We therefore conclude that silicate perovskite can integrate large amounts of ferric iron, even in an Al_2O_3-free system, reaching a composition of stoichiometry probably close to $Ca_3Fe_2Si_3O_{12}$ (Wang et al. 1999). We estimate that this Fe^{III}-rich perovskite would be unstable in the presence of an excess of MgO, because Fe_2O_3 would probably react with the magnesiowüstite to form the $CaMn_2O_4$-form of $MgFe_2O_4$. It is

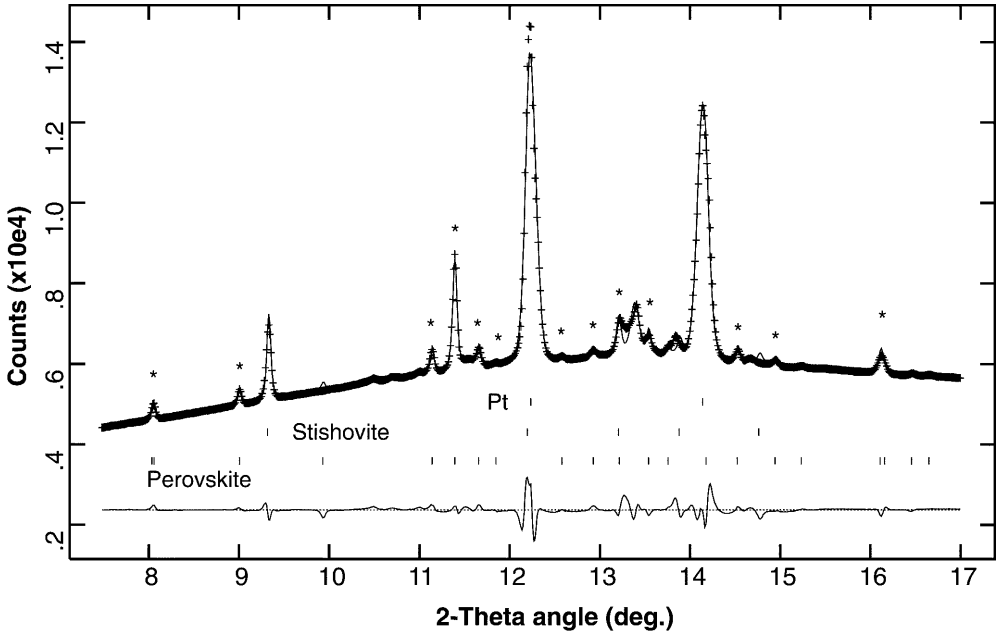

Fig. 6 Lebail refinement of the diffraction pattern recorded at 63 GPa after YAG laser annealing for the same sample as presented in Fig. 5. Note the significant decrease in intensity of the stishovite lines. All features can be explained by the occurrence of a Pbnm perovskite, stishovite, and Pt. For this system, the lack of hematite diffraction lines evidences the formation of a perovskite phase with composition intermediate between Fe_2O_3 and $MgSiO_3$, with stoichiometry probably close to $Mg_3Fe_2Si_3O_{12}$

indeed well documented that the presence of Al^{3+} is usually required to increase the silicate perovskite Fe^{III} content in perovskite–magnesiowustite assemblages.

Acknowledgements We thank G. Fiquet, T. le Bihan, M. Mezouar, and S. Bauchau for help during experiments on ID30, and N. Funamori for a fruitful review. This work is no. 264 IT-CNRS and no. 1732 IPGP contribution.

References

Akaogi M, Hamada Y, Suzuki T, Kobayashi M, Okada M (1999) High-pressure transitions in the system $MgAl_2O_4$–$CaAl_2O_4$: a new hexagonal aluminous phase with implication for the lower mantle. Phys Earth Planet Int 115: 67–77

Anderson OL, Isaak DG, Yamamoto S (1989) Anharmonicity and the equation of state for gold. J Appl Phys 65: 1534–1543

Andrault D, Fiquet G, Guyot F, Hanfland M (1998a) Pressure-induced landau-type transition in stishovite. Science 23: 720–724

Andrault D, Fiquet G, Itie J-P, Richet P, Gillet Ph, Häusermann D, Hanfland M (1998b) Pressure in a laser-heated diamond-anvil cell: implications for the study of Earth's interior. Eur J Mineral 10: 931–940

Fei Y, Frost DJ, Mao H-K, Prewitt CT, Häusermann D (1999) In situ structure determination of the high-pressure phase of Fe_3O_4. Am Mineral 84: 203–206

Funamori N, Jeanloz R, Nguyen JH, Kavner A, Cadwell WA, Fujino K, Miyajima N, Shinmei T, Tomioka N (1998) High-pressure transformation in $MgAl_2O_4$. J Geophys Res 103: 20813–20818

Gerward L, Ohen JS (1995) High-pressure studies of magnetite and magnesioferrite using synchrotron radiation. Appl Rad Isotop 46: 553–554

Hammersley J (1996) Fit2d user manual. ESRF publication, Grenoble, France

Hazen RM, Downs RT, Finger LW (1993) Crystal chemistry of ferromagnesian spinels: evidence for Mg-Si disorder. Am Mineral 78: 1320–1323

Häusermann D, Hanfland M (1996) Optics and beamlines for high-pressure research at the European synchrotron radiation facility. High Press Res 14: 223–234

Irifune T, Fujino K, Ohtani E (1991) A new high-pressure form of $MgAl_2O_4$. Nature 349: 409–411

Ito E, Takahashi E (1989) Postspinel transformations in the system Mg_2SiO_4–Fe_2SiO_4 and some geophysical implications. J Geophys Res 94: 10637–10646

Jamieson J, Fritz J, Manghnani M (1982) Pressure measurement at high temperature in X-ray diffraction studies: gold as a primary standard. In: Akimoto S, Manghnani MH (eds) High-pressure research in geophysics. Center for Academic Publishers, Tokyo, pp 27–48

Larson AC, Von Dreele RB (1998) GSAS manual. Los Alamos National Laboratory publication, LAUR 86–748

Lauterbach S, McCammon CA, van Aken P, Langenhorst F, Seifert F (2000) Mössbauer and ELNES spectroscopy of (Mg, Fe)(Si,Al)O_3 perovskite: a highly oxidized component of the lower mantle. Contrib Mineral Petrol 138: 17–26

Liu LG (1975) Disproportionation of $MgAl_2O_4$ spinel at high pressures and temperatures. Geophys Res Lett 41: 398–404

McCammon CA, Rubie DC, Ross II CR, Seifert F, O'Neill HS (1992) Mössbauer spectra of $^{57}Fe_{0.05}Mg_{0.95}SiO_3$ perovskite at 80 and 298 K. Am Mineral 77: 894–897

Ohtaka O, Tobe H, Yamanaka T (1997) Phase equilibria for the Fe_2SiO_4–Fe_3O_4 system under high pressure. Phys Chem Miner 24: 555–560

Oikawa K, Kamiyama T, Izumi F, Chakoumakos BC, Ikuta H, Wakihara M, Li-Jianqi, Matsui Y (1998) Structural phase transition of the spinel-type oxide $LiMn_2O_4$. Solid State Ionics, Diffusion Reactions 109: 35–41

Reid AF, Ringwood AE (1969) Newly observed high pressure transformations in Mn_3O_4, $CaAl_2O_4$, and $ZrSiO_4$. Earth Planet Sci Lett 6: 205–208

Staun Olsen J, Cousins CS, Gerward L, Jhans H, Sheldon BJ (1991) A study of the crystal structure of Fe_2O_3 in the pressure range up to 65 GPa using synchrotron radiation. Physica Scripta 43: 327–330

Thoms R, Bauchau S, Kunz M, Le Bihan T, Mezouar M, Häusermann D, Strawbridge D (1998) An improved detector for use at synchrotrons. Nucl Instr Meth (A)413: 175–180

Wang ZW, Yagi T, Kondo T (1999) Pressure-induced phase transformation and amorphization in $Ca_3Fe_2Si_3O_{12}$: a high-pressure X-ray diffraction study. J Phys Chem Solids 60: 441–444

Woodland AB, Angel RJ, Koch M, Kunz M, Miletich R (1999) Equations of state for $Fe_3^{2+}Fe_3^{2+}Fe_3^{2+}Si_3O_{12}$ "skiagite" garnet and Fe_2SiO_4-Fe_3O_4 spinel solid solutions. J Geophys Res 104: 20049–20058

Yagi T, Akimoto S (1982) Rapid X-ray measurements to 100 GPa Range and static compression of Fe_2O_3. In: Akimoto S, Manghnani MH (eds) High-pressure research in geophysics. Center for Academic Publishers, Tokyo

Yutani M, Yagi T, Yusa H, Irifune T (1997) Compressibility of calcium ferrite-type $MgAl_2O_4$. Phys Chem Miner 24: 340–344